JACS
JOURNAL OF THE AMERICAN CHEMICAL SOCIETY
Communication
pubs.acs.org/JACS

When Electron Transfer Meets Electron Transport in Redox-Active Molecular Nanojunctions

Marion Janin, Jalal Ghilane,* and Jean-Christophe Lacroix*

NanoElectroChemistry Group, Université Paris Diderot, ITODYS, UMR 7086 CNRS, 75205 Paris Cedex 13, France

Supporting Information

ABSTRACT: A scanning electrochemical microscope (SECM) was used to arrange two microelectrodes face-to-face separated by a micrometric gap. Polyaniline (PANI) was deposited electrochemically from the SECM tip side until it bridged the two electrodes. The junctions obtained were characterized by following the current through the PANI as a function of its electrochemical potential measured versus a reference electrode acting as a gate electrode in a solid-state transistor. PANI nanojunctions showed conductances below 100 nS in the oxidized state, indicating control of the charge transport within the whole micrometric gap by a limited number of PANI wires. The SECM configuration makes it possible to observe in the same experiment and in the same current range the electron-transfer and electron-transport processes. These two phenomena are distinguished here and characterized by following the variation of the current with the bias voltage and the scan rate. The electron-transfer current changes with the scan rate, while the charge-transport current varies with the bias voltage. Finally, despite the initially micrometric gap, a junction where the conductance is controlled by a single oligoaniline strand is achieved.

The electrical properties of single molecules or of a small number of molecules are of heightened interest because of potential applications in molecular electronics and new opportunities for understanding charge transport in organic systems.[1] Various methods have been proposed for measuring conductance through molecules, including scanned-probe techniques,[2] mercury-drop electrodes,[3] electrical or mechanical break junctions,[4,5] sandwich electrodes,[6] and top contact on self-assembled monolayers.[7] Recently, there has been a surge of interest in redox-active molecules. Indeed, in molecular electronics one wishes to electrically wire one or a few redox molecules between two electrodes and to control charge transport across this or these molecule(s) by switching its/their redox state using an electron-transfer process.[8,9] In order to do so in a solid-state device, a third electrode, acting as a gate, has to be placed a few nanometers from the molecule, which is not a trivial task.[10] To overcome this difficulty, performing the experiment in an electrolyte and controlling the potential with respect to a reference electrode, as in the case of conventional electrochemistry, appears to be a good compromise. This electrochemical gate method has been employed to control charge transport in conducting polymers and nanojunctions,[11] carbon nanotubes,[12] and redox molecules.[9,13] In the case of a p-dopable conjugated oligomer, an electrochemical gate-induced conductance increase is due to the switching of the oligomer from the reduced (low conductance) state to the oxidized (high conductance) state.[9a] This picture is supported by the fact that the oxidation of the oligomer is accompanied by a decrease in the HOMO−LUMO gap[13c] and was at the origin of Aviram's proposal based on electroactive oligothiophenes.[1b]

In such a scheme, redox-gated electron transfers among the few molecules making the junction is a transient process. Ultimately, one electron can in theory be used to write the redox state of a single-molecule device. The current associated with this process is thus very small.[14] In contrast, electron transport across the junction is a steady-state reading process involving many electrons crossing the few (or the single) molecules of the junction.[9] As a consequence, it is not possible or it is very difficult to observe electron transfer and electron transport in the same experiment using a molecular junction involving a few molecules.

We report here a study using highly stable polyaniline redox-active nanojunctions where fewer than 10 oligoaniline strands control the charge transport between the two electrodes, obtained using scanning electrochemical microscopy (SECM)[15] and two micrometric tips facing each other (5 μm radius). The junctions were investigated by following the variation of the current at the tips or through the PANI as a function of the gate potential at fixed tip1/tip2 bias voltage. With this configuration it is possible to easily separate and study the electrochemical response of the deposited PANI, and the electron transport through the PANI, using various biases and scan rates values.

A four-electrode setup operating in scanning electrochemical configuration SECM was used. Two ultramicroelectrodes (UMEs) were used as the working electrode (tip1) and the substrate (tip2) (Figure SI1). When a polyaniline connects tip1 and tip2, as for a solid-state transistor, the variation of the tip1−tip2 (source−drain) current versus the gate ($E_{tip1} - E_{ref} = V_g$) potential is recorded. The two tip potentials are scanned simultaneously, while a fixed bias ($E_{tip2} - E_{tip1} = V_{SD}$) is maintained between the two electrodes. Negative interelectrode bias corresponds to a situation where tip2 is at a lower electrochemical potential than tip1. Other experimental details are given in the Supporting Information.

Figure 1 shows the response of one PANI junction with a fixed interelectrode bias, $E_{tip2} - E_{tip1} = -20$ mV. The black and red curves show that below 0.2 V/SCE the junction is in an insulating

Received: December 14, 2012
Published: January 18, 2013

dx.doi.org/10.1021/ja3122125 | J. Am. Chem. Soc. 2013, 135, 2108−2111

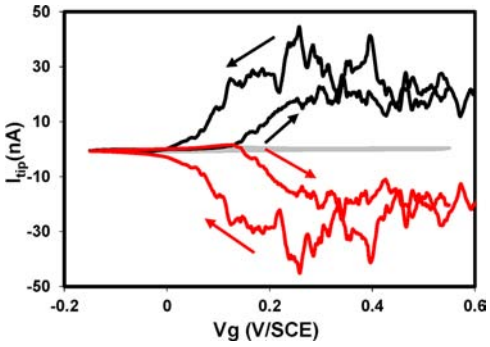

Figure 1. I_{tip} as a function of the gate voltage using −20 mV interelectrode bias and a scan rate of 0.1 V/s: black, tip1; red, tip2; gray, electrochemical response of the PANI film at tip1 when tip2 is unbiased.

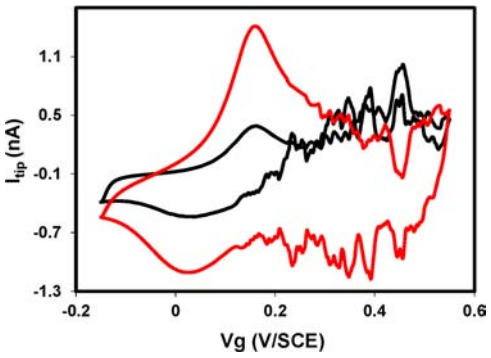

Figure 2. I_{tip} as a function of the gate voltage using −20 mV bias and a scan rate of 0.1 V/s: black, tip1; red, tip2.

state and no current (or leakage current in the pA range) is flowing between the two electrodes. Next, the current starts to increase, where PANI starts to be oxidized, and reaches a maximum at 0.4 V. During the backward scan the PANI junction is reversibly switched from the conducting to the insulating state. However, the reverse scan shows a hysteresis induced by structural relaxation of the junction.

The use of two UMEs facing each other makes it possible to observe simultaneously the current at both tips and thus to use their relative values, their signs, and their fluctuations to separate electron transfer from electron transport in the overall signal, in marked contrast with the situation when a tip and a large substrate are used. In the latter situation current at the substrate is dominated by leakage and double-layer capacitance and cannot be linked to the current crossing the UME tip.

In the present case, the curves recorded at tip1 and tip2 exhibit a perfect symmetry, with $I_{tip1} = -I_{tip2}$ and $\Delta I_{tip1} = -\Delta I_{tip2}$ (ΔI_{tip} being the variation of a tip current with time or with small gate potential increments). This clearly shows that these two currents, reaching 20 nA around 0.4 V during the forward scan, are due to charge transport across the PANI junction. In contrast, when tip2 is unbiased, the current versus gate voltage curve is that of PANI electroactivity (Figure SI2), with a current flowing between the tips and the counter electrode in the nA range (total amount of PANI involved in the switching process can be evaluated to 10^{+10} electroactive sites) and associated with the electron transfer (doping/de-doping processes, I_{gate}). The current due to electron transfer used for doping the polymer is thus at least 1 order of magnitude smaller than that due to electron transport across the junction when a −20 mV interelectrode bias is applied (I_{gate} is negligible compared to I_{SD}). Overall, the junction behaves as a transistor (source−drain current $I_{SD} = I_{tip1} = -I_{tip2}$, $V_g = E_{tip1} - E_{ref}$ triggering the transport properties). From Figure 1 one can calculate a 1 μS conductance of the junction in its conducting state (V_g = 0.4 V/SVE). In addition, current fluctuations appear when the PANI starts to be conducting, while they disappear in its insulating state. Such fluctuations have already been observed and were attributed to on/off redox switching of a limited number of oligomer strands.[16]

A number of junctions, reducing the amount of PANI wire reaching the tip2, were created and characterized. Figure 2 presents the variation of the current versus the electrochemical potential of a new junction at −20 mV interelectrode bias recorded at tip1 and at tip2. (Note that such junctions were reproducibly generated.) The shape of the curves differs from that observed in Figure 1. For potentials below 0.2 V/SCE the shape is similar to that obtained for the cyclic voltammogram of PANI with an oxidation peak at 0.15 V/SCE. The peak shape corresponds to the electrochemical doping of the PANI wires. These observations are valid for both tip1 and tip2. In this potential range, the values of I_{tip1} and I_{tip2} are no longer equal, and the difference corresponds to the amount of PANI deposited on each electrode. Both currents have the same sign, and electrons are flowing between each tip and the counter electrode. Note that the total amount of PANI involved in the switching process is close to that of Figure 1 (10^{+10} electroactive sites). Beyond 0.2 V/SCE, current fluctuations became visible and the direction of the fluctuations is inverted when I_{tip1} and I_{tip2} are compared, with $\Delta I_{tip1} = -\Delta I_{tip2}$. This indicates that tip1 and tip2 are connected through a PANI junction making a new current flow through the junction and adding to or subtracting from the current due to the electrochemical doping. In contrast to the previous junction, the current associated with electron transfer (I_{gate}) leading to doping is no longer negligible compared to the electron-transport current within the junction. Indeed, the electrochemical doping/de-doping process is observed here first and is followed by current transport adding to the signal. This process appears reversible since, during the backward potential sweep, fluctuations first disappear and a PANI reduction peak can be easily seen. The same behavior is observed when multiple potential cycles are used, which indicates that the junction is stable and that a permanent PANI wire connects tip1 and tip2.

Figure 3a shows the overlay of the characterization of the junction performed at −20 mV interelectrode bias (black) and when tip2 is unbiased (gray). Figure 3b shows the conductance variation as a function of the gate voltage during the backward potential sweep (de-doping process) after removal of the electrochemical signal. Decreasing the gate potential from 0.55 to 0.4 V leads to an enhancement of the conductance, and a maximum is reached at 0.4 V. It is followed by a conductance decrease due to the reduction of the junction. The conductance

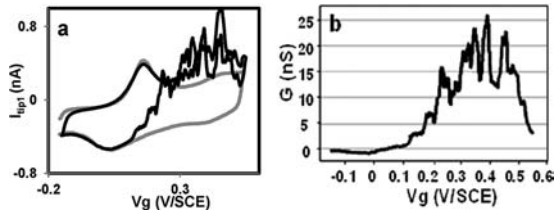

Figure 3. (a) (Black) I_{tip1} current as a function of the gate voltage using −20 mV bias; (gray) cyclic voltamogram at tip1 when tip2 (substrate) is unbiased. (b) Conductance variation as a function of potential after elimination of the electrochemical process.

dx.doi.org/10.1021/ja3122125 | J. Am. Chem. Soc. 2013, 135, 2108−2111

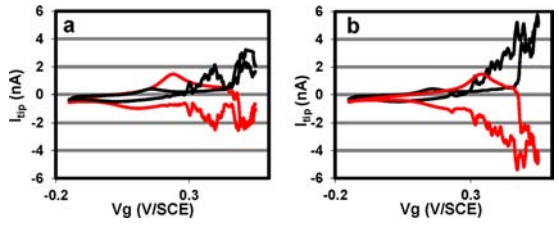

Figure 4. Currents I_{tip1} (black) and I_{tip2} (red) as a function of the electrochemical potential (gate voltage V_g) for PANI junction at different biases: (a) −100 and (b) −200 mV.

of the junction in the oxidized state, around 0.4 V/SCE, is about 30−50 nS during the backward scan and between 20 and 40 nS during the forward scan. Compared to the conductance of heptaaniline in a single-molecule setup in the oxidized state (5 nS),[17] this value corresponds to a junction where fewer than 10 oligoaniline strands control the charge transport between the two electrodes. Furthermore, the last conductance change in the dedoping process occurs stepwise with 5 nS step height, suggesting that each step reflects the conductance of a single oligoaniline strand. This shape has been already observed and was clearly presented as a signature of single-molecule events.[16,18]

The advantage of the generated junctions is their large time stability, allowing us to perform successive electrochemical measurements, with the same junction, without significant change in the conductance. Based on this stability, the same junction has been investigated using multiple cycles (Figure SI3), various interelectrode bias voltages, and various scan rates.

Figure 4 shows the variation of tip1 and tip2 current as a function of the gate voltage recorded at different bias voltages, −100 and −200 mV. Figure SI4 shows the overlay of the tip1 current using various bias voltages for the same junction and thus includes the results reported in Figure 2 for −20 mV bias. Overall, and whatever the applied bias, during the forward scan a peak shape corresponding to the electrochemical oxidation of the PANI deposited at tip1 and tip2 is observed. Both currents (I_{tip1} and I_{tip2}) have the same direction (anodic current) but not the same value. Following this, electron transport through the junction is observed, as attested by several features: an abrupt increase in the current, a change in the current direction with $\Delta I_{tip1} = -\Delta I_{tip2}$, and the appearance of fluctuations.

Analysis of the obtained data using different bias voltages reveals various features. For the electron-transfer process related to the electrochemical doping/de-doping: (i) the peak intensity and direction corresponding to the electrochemical doping/dedoping of the PANI film remain unchanged when the value of the bias voltage is varied; (ii) the peak potential at tip2 is shifted by the value of the applied bias compared to that at tip1. As expected, the variation of the bias voltage does not affect the electrochemical process, since it only controls the current flowing between tip1 or tip2 and the counter electrode. For the part representing electron transport through the junction: (i) increase in the bias value enhances the current through the PANI junction; (ii) perfect symmetry between tip1 and tip2 in terms of current fluctuations is recorded ($\Delta I_{tip1} = -\Delta I_{tip2}$). The conductance of the junction in the oxidized state during the forward scan remains around 20−30 nS, suggesting control of the electron transport in the entire junction by less than 10 oligoaniline strands.

Another parameter leading to differentiate between electrochemically induced electron transfer and transport measurements is the dependence of the associated currents on the scan

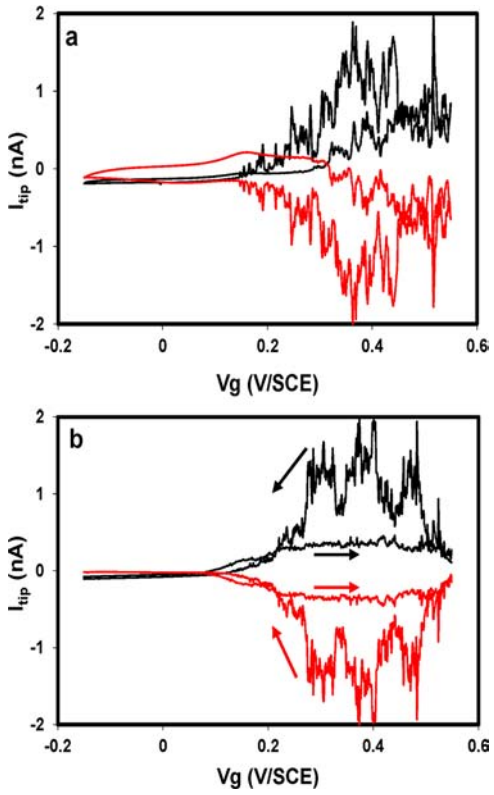

Figure 5. Charge-transport current as a function of the electrochemical potential (gate voltage V_g) for polyaniline junction at different scan rates using a −20 mV bias voltage: (a) 10 and (b) 1 mV/s.

rate. Figure 5 shows the current variation at tip1 (black line) and tip2 (red line) versus the potential, using different scan rates and fixed bias (−20 mV). Independently on the used scan rate all the data show similar behavior. For a potential below 0.2 V/SCE, the current is governed by the electrochemical process (peak shape). Beyond this potential charge transport through the PANI junction contributes to the measured current, as attested by the inversion of the current direction (red curve) and the appearance of fluctuations with $\Delta I_{tip1} = -\Delta I_{tip2}$. The oxidation and reduction peaks vary linearly with the scan rate. In contrast, the current related to charge transport remains unchanged when varying the scan rate, in the range of 0.4−0.7 nA in the forward scan. As a result, the conductance of the PANI junction in the oxidized state is again around 20−35 nS. When a higher scan rate, 1 V/s, is used, it appears that only electrochemical current is observed (Figure SI5). In this case electron transport is not observed because the electrochemical current becomes 10 times higher than the electron transport. After this experiment, lowering the scan rate to 0.1 V/s leads to recovery of the signal with an electrochemical signal followed by the electron transport and a conductance in the 20−30 nS range, indicating that the PANI is still connecting the two electrodes. This value is similar to that measured previously, highlighting the large time stability of the generated PANI junction even after several electrochemical measurements. Overall, the same redox-active nanojunctions where fewer than 10 oligoaniline strands control the charge transport were stable enough to be studied during more than 1 h. Such stability exceeds those of all the previous systems reported to date.

Finally, we discuss the possibility of reaching a single-molecule regime based on the SECM configuration. Thanks to the piezomotor, SECM makes it possible to shrink the junctions by simply

dx.doi.org/10.1021/ja3122125 | J. Am. Chem. Soc. 2013, 135, 2108−2111

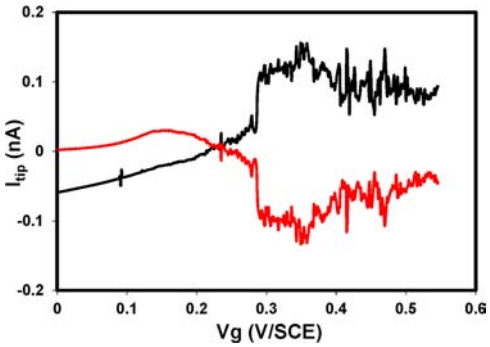

Figure 6. Charge-transport current as function of electrochemical potential (gate voltage V_g) for polyaniline junction using −20 mV bias voltage: black, tip1; red, tip2. Scan rate 1 mV/s.

withdrawing the SECM tip. The latter junction was submitted to elongation by moving up the tip1. After this process the variation of tip1 (black line) and tip2 (red line) current versus the potential using −20 mV bias was recorded (Figure 6). First, the electrochemical oxidation of PANI for both tip1 and tip2 is observed at 0.15 V (more easily observed on tip2 red curve). In this case a scan rate of about 1 mV/s has been used. The use of such a low scan rate decreases the current intensity of the peak related to the electrochemical process. For a potential below 0.25 V/SCE, both currents (tip1 and tip2) have the same direction and the current at tip2 (red curve) is higher than that at tip1 (black curve), which is related to the difference in the amount of PANI deposited at each electrode. For a potential above 0.25 V/SCE, an abrupt jump in the current related to electron transport through the junction is observed and stabilizes at a value of about 0.1 nA. Perfect symmetry, with $\Delta I_{tip1} = -\Delta I_{tip2}$, is observed between the current recorded at tip1 (black) and tip2 (red), indicating that current is governed by the charge-transport process through the PANI nanowires. The conductance in the oxidized state of the junction here is around 5 nS. Compared to the reported conductance for a single oligoaniline using the STM setup,[17] this value suggests that electron transport within the whole PANI junction is controlled by a single oligoaniline strand. The use of the SECM configuration starting with two UMEs leads to the observation of single-molecule events despite the μm gap size used.

In summary, scanning electrochemical microscopy , where two microelectrodes are placed face-to-face separated by a micrometric gap, has been successfully used for the fabrication of redox-gated junctions. Highly stable and reversible redox-gated nanojunctions were routinely obtained with conductances in the 10^{-7}−10^{-8} S range. More interestingly, separate electron-transfer and electron-transport processes in such a redox-gated nanojunction has been clearly observed and characterized for the first time. The high stability of the generated PANI nanojunction makes it possible to clearly distinguish between these two different processes. Despite the fact that fewer than 10 strands are involved in the junction, changing the scan rate affects only the electron-transfer current, while changing the bias voltage has an influence on the charge-transport current. Finally, based on the same setup, a PANI junction where charge transport is controlled by a single oligoaniline strand has been obtained.

■ ASSOCIATED CONTENT

Ⓢ Supporting Information

Experimental methods, figures, and results. This material is available free of charge via the Internet at http://pubs.acs.org.

■ AUTHOR INFORMATION

Corresponding Author

lacroix@univ-paris-diderot.fr; jalal.ghilane@univ-paris-diderot.fr

Notes

The authors declare no competing financial interest.

■ REFERENCES

(1) (a) Yaliraki, S. N.; Kemp, M.; Ratner, M. A. *J. Am. Chem. Soc.* **1999**, *121*, 3428. (b) Aviram, A.; Ratner, M. *Chem. Phys. Lett.* **1974**, *29*, 277. (c) Ratner, M. A.; Davis, B.; Kemp, M.; Mujica, V.; Roitberg, A.; Yaliraki, S. *Ann. N.Y. Acad. Sci.* **1998**, 852. (d) Lacroix, J. C.; Chane-Ching, K. I.; Maquère, F.; Maurel, F. *J. Am. Chem. Soc.* **2006**, *128*, 7264. (e) Curtis, C. L.; Ritchie, J. E.; Sailor, M. J. *Science* **1993**, 2014.

(2) Xu, B.; Tao, N. J. *Science* **2003**, *301*, 1221.

(3) Haag, R.; Rampi, M. A.; Holmlin, R. E.; Whitesides, G. M. *J. Am. Chem. Soc.* **1999**, *121*, 7895.

(4) Kergueris, C.; Bourgoin, J. P.; Palacin, S.; Esteve, D.; Urbina, C.; Magoga, M.; Joachim, C. *Phys. Rev. B* **1999**, *59*, 19.

(5) Reed, M. A.; Zhou, C.; Muller, C. J.; Burgin, T. P.; Tour, J. M. *Science* **1997**, *278*, 252.

(6) Kushmerick, J. G.; Naciri, J.; Yang, J. C.; Shashidhar, R. *Nano Lett.* **2003**, *3*, 897.

(7) (a) Chabinyc, M. L.; Chen, X.; Holmlin, R. E.; Jacobs, H.; Skulason, H.; Frisbie, C. D.; Mujica, V.; Ratner, M. A.; Rampi, M. A.; Whitesides, G. M. *J. Am. Chem. Soc.* **2002**, *124*, 11730. (b) McCreery, R. L.; Dieringer, J.; Solak, A. O.; Snyder, B.; Nowak, A. M.; McGovern, W. R.; DuVall, S. *J. Am. Chem. Soc.* **2003**, *125*, 10748. (c) Martin, P.; Della Rocca, M. L.; Anthore, A.; Lafarge, P.; Lacroix, J. C. *J. Am. Chem. Soc.* **2012**, *134*, 154.

(8) (a) Nitzan, A.; Ratner, M. A. *Science* **2003**, *300*, 1384. (b) He, H. X.; Li, C. Z.; Tao, N. J. *Appl. Phys. Lett.* **2001**, *78*, 811. (c) Choi, S. H.; Kim, B.; Frisbie, D. C. *Science* **2008**, *320*, 1482.

(9) (a) Lindsay, S.; Ratner, M. A. *Adv. Mater.* **2007**, *19*, 23. (b) Ulgut, B.; Abruña, H. D. *Chem. Rev.* **2008**, *108*, 2721.

(10) (a) Di Ventra, M.; Pantelides, S. T.; Lang, N. D. *Appl. Phys. Lett.* **2000**, *76*, 3448. (b) Damle, P.; Rakshit, T.; Paulssom, M.; Datta, S. *IEEE Trans. Nanotech.* **2002**, *1*, 145.

(11) (a) Paul, E. W.; Ricco, A. J.; Wrighton, M. S. *J. Phys. Chem.* **1985**, *89*, 1441. (b) White, H. S.; Kittlesen, G. P.; Wrighton, M. S. *J. Am. Chem. Soc.* **1984**, *106*, 5375.

(12) Rosenblatt, S.; Yaish, Y. P.; Park, J.; Gore, J.; Sazonova, V.; McEuen, P. L. *Nano Lett.* **2002**, *2*, 869.

(13) (a) Tao, N. J. *Phys. Rev. Lett.* **1996**, *76*, 4066. (b) Gittins, D. I.; Bethell, D.; Schiffrin, D. J.; Nichols, R. J. *Nature* **2000**, *408*, 67. (c) Xu, B.; Xiao, X.; Yang, X.; Zang, L.; Tao, N. J. *J. Am. Chem. Soc.* **2005**, *127*, 2386. (d) Chen, F.; He, J.; Nuckolls, C.; Roberts, T.; Klare, J. E.; Lindsay, S. *Nano Lett.* **2005**, *5*, 503. (e) Xiao, X.; Brune, D.; He, J.; Lindsay, S. M.; Gorman, C. B.; Tao, N. J. *Chem. Phys.* **2006**, *326*, 138. (f) Chen, F.; Tao, N. J. *Acc. Chem. Res.* **2009**, *42*, 429. (g) Zhou, X. S.; Liu, L.; Fortgang, P.; Lefevre, A. S.; Serra-Muns, A.; Raouafi, N.; Amatore, C.; Mao, B. W.; Maisonhaute, E.; Schöllhorn, B. *J. Am. Chem. Soc.* **2011**, *133*, 7509.

(14) (a) Fan, F.-R.; Kwak, J.; Bard, A. J. *J. Am. Chem. Soc.* **1996**, *118*, 9669. (b) Fan, F.-R. F.; Bard, A. J. *Science* **1997**, *277*, 1791.

(15) Janin, M.; Ghilane, J.; Randriamahazaka, H.; Lacroix, J. C. *Anal. Chem.* **2011**, *83*, 9709.

(16) (a) He, H. X.; Zhu, J. S.; Tao, N. J.; Nagahara, L. A.; Amlani, I.; Tsui, R. *J. Am. Chem. Soc.* **2001**, *123*, 7730. (b) He, H. X.; Li, X. L.; Tao, N. J.; Nagahara, L. A.; Amlani, I.; Tsui, R. *Phys. Rev. B* **2003**, *68*, 045302.

(17) Chen, F.; He, J.; Nuckolls, C.; Roberts, T.; Klare, J.; Lindsay, S. *Nano Lett.* **2005**, *5*, 503.

(18) (a) Xiao, X. Y.; Nagahara, L. A.; Rawlett, A. M.; Tao, N. J. *J. Am. Chem. Soc.* **2005**, *127*, 9235. (b) Xu, B. Q.; Li, X. L.; Xiao, X. Y.; Sakaguchi, H.; Tao, N. J. *Nano Lett.* **2005**, *5*, 1491.